Biochemistry and Biophysics Reports 28 (2021) 101148

Contents lists available at ScienceDirect

Biochemistry and Biophysics Reports

journal homepage: www.elsevier.com/locate/bbrep

Analysis of signal components < 500 Hz in brain organoids coupled to microelectrode arrays: A reliable test-bed for preclinical seizure liability assessment of drugs and screening of antiepileptic drugs

R. Yokoi, M. Shibata, A. Odawara, Y. Ishibashi, N. Nagafuku, N. Matsuda, I. Suzuki *

Department of Electronics, Graduate School of Engineering, Tohoku Institute of Technology, 35-1 Yagiyama Kasumicho, Taihaku-ku, Sendai, Miyagi, 982-8577, Japan

ARTICLE INFO

Keywords:
Cerebral organoid
Microelectrode array
Frequency component
Seizure liability of drug
Antiepileptic drug
In vitro to *in vivo* extrapolation

ABSTRACT

Brain organoids with three-dimensional structure and tissue-like function are highly demanded for brain disease research and drug evaluation. However, to our knowledge, methods for measuring and analyzing brain organoid function have not been developed yet. This study focused on the frequency components of an obtained waveform below 500 Hz using planner microelectrode array (MEA) and evaluated the response to the convulsants pentylenetetrazol (PTZ) and strychnine as well as the antiepileptic drugs (AEDs) perampanel and phenytoin. Sudden and persistent seizure-like firing was observed with PTZ administration, displaying a concentration-dependent periodic activity with the frequency component enhanced even in one oscillation characteristic. On the other hand, in the administration of AEDs, the frequency of oscillation decreased in a concentration-dependent manner and the intensity of the frequency component in one oscillation also decreased. Interestingly, at low doses of phenytoin, a group of synchronized bursts was formed, which was different from the response to the perampanel. Frequency components contained information on cerebral organoid function, and MEA was proven useful in predicting the seizure liability of drugs and evaluating the effect of AEDs with a different mechanism of action. In addition, frequency component analysis of brain organoids using MEA is an important analysis method to perform *in vitro* to *in vivo* extrapolation in the future, which will help explore the function of the organoid itself, study human brain developments, and treat various brain diseases.

1. Introduction

Organoids are three-dimensional cell aggregates *in vitro*, capable of self-renewal or self-organization and exhibit organ-like tissue functions [1]. They are derived from pluripotent stem cells or isolated organ progenitors in humans. Recently, *in vitro* to *in vivo* extrapolation (IVIVE), which is explaining and predicting *in vivo* phenomena from *in vitro* findings, has become a useful approach. Therefore, such extrapolation can be guaranteed when using organoids that are close to the structure of living organisms and have the potential for biomedical applications and personalized medicine [2]. To date, organoids have been established for the human brain, stomach, retina, esophagus, lung, liver, prostate, ovary, intestine, kidney, and pancreas [3,4]. Human brain organoids are remarkably high-degree models of early embryonic and fetal brain development as well as human-specific diseases [5]. Organoids with the characteristics of the hippocampus [6], midbrain [7], hypothalamus [8], cerebellum [9], and anterior pituitary [10] have already been developed.

Seizures are defined as an abnormal excitement of the brain activity and are a serious side effect of various medications [11,12]. During the preclinical stage of drug development, it is necessary to develop a highly accurate method to predict the seizure liability of the candidate drug that can be extrapolated to humans. In the field of drug discovery, as well as safety pharmacology of drugs, the development of new antiepileptic drugs (AEDs) is required urgently [13]. The use of human-induced pluripotent stem cells (iPSCs) can be extrapolated to humans. A method for predicting the seizure liability of drugs using the microelectrode array (MEA) method for cultured human iPSC-derived neurons has been reported [14–16]. However, because cultured human iPSC-derived neurons have a random structure, the use of cerebral organoids is considered an effective method for approaching extrapolation *in vivo*.

In recent years, the electrical activities in organoids have been

Abbreviations: MEA, microelectrode array; PTZ, pentylenetetrazol; AEDs, antiepileptic drugs; EEG, electroencephalography; IVIVE, *in vitro* to *in vivo* extrapolation.

* Corresponding author.
E-mail address: i-suzuki@tohtech.ac.jp (I. Suzuki).

https://doi.org/10.1016/j.bbrep.2021.101148
Received 7 July 2021; Received in revised form 3 October 2021; Accepted 4 October 2021

reported using planner MEA [17–22]. For the functional measurement of organoids, single unit, multiunit, field potential, synaptic current recording, etc., can be selected according to the aim of the analysis. The method can also be selected according to the purpose, such as the silicon probe, MEA, Ca^{2+} imaging, and patch clamp methods. In the case of organoid measurement using planner MEA, organoids can be efficiently measured with high throughput by simply placing the organoid on MEA, which is an effective method for toxicity assessment of drugs and drug discovery screening. Multiunit analysis is mainstream for organoid measurement using planner MEA, but frequency component analysis of the field potential is also considered effective. If the response of the frequency components to compounds can be detected from organoids, they have the potential to be an effective index to assess the seizure liability of drugs and functional evaluation in the development of new AEDs. In the future, it is expected to be compared with *in vivo* EEG, which can record field potential. In the analyses of *in vivo* EEGs of seizures, the frequency band below 500 Hz is typically analyzed [23,24].

Therefore, for *in vitro* cerebral organoids, activity characteristics are considered inherent in the frequency component below 500 Hz and may be changed by the administration of convulsants and AEDs. In this study, we investigated the frequency component obtained from cerebral cortical organoids using planner MEA. Furthermore, we observed changes in activity following the administration of convulsants and AEDs.

2. Materials and methods

2.1. Human iPSC-derived cerebral organoid culture

Healthy human-derived iPSCs (201B7) were obtained from the Institute of Physical and Chemical Research. Briefly, iPSCs were cultured by StemFit (AK02 N, Ajinomoto) and were collected using Gentle Cell Dissociation Reagent (ST-07174, STEMCELL Technologies) when cells were *confluent* on six well dishes. Collected cells were centrifuged for 5 min at 800 rpm at room temperature. After discarding the supernatant, 1 ml EB seeding medium (EB formation medium added 10 mM Y-27632) was added and the cell pellet was resuspended. iPSCs were cultured at 9.0×10^3 cells/wel in 96 wells using the EB seeding medium. After 2 and 4 days, 100 μl EB seeding medium was added per well. On day 5, organoids were observed and spherical form samples were selected. EB seeding medium was substituted with an induction medium and incubated for 2 days. Organoids were embedded in Matrigel (354,277, Corning) and incubated in an expansion medium for 3 days. The expansion medium was substituted with a maturation medium, and the organoids were incubated in an orbital shaker (COSH6, AS ONE Corporation). Organoids were maintained in the maturation medium for 3 months, with medium replenishment performed every 3–4 days. After 3 months, the culture medium was changed to Brain Phys (ST-05792, STEMCELL Technologies). The Medium of the STEMdiff Cerebral Organoid Kit (ST-08570, STEMCELL Technologies) was used for organoid formation.

2.2. Immunostaining

Cerebral organoids were fixed with 4% *paraformaldehyde* in PBS. The samples were embedded in Optimal Cutting Temperature Compound (45,833, Sakura Finetek Japan) and sectioned at a thickness of 10 μm using Leica CM3050 S Cryostat. Organoid sections were permeabilized and blocked with blocking solution (0.05% Triton X-100 and 5% goat serum in PBS). Primary antibodies in blocking solution were then added and incubated at 4 °C for overnight, followed by washing and incubation with secondary antibodies. The following antibodies were used—primary antibodies: rabbit anti-pax6 antibody (ab5790, Abcam), mouse anti-β-tubulin III antibody (ab7751, Abcam), and rat anti-ctip2 antibody (ab18465, Abcam) and secondary antibodies: donkey antirat (ab150155, Abcam), donkey antimouse, (A10036, Invitrogen), and donkey antirabbit, (A21206, Invitrogen). Images were viewed using a confocal microscope (TCS SP8, Leica). The image intensity was adjusted using the ImageJ software (NIH).

2.3. Microelectrode array recording and multiunit analysis

The MEA experiment was performed following a previously described method [15]. At 4 months, the cerebral organoids were mounted on a 24-well planner MEA chip. Spontaneous activities in organoids were acquired at 37 °C and 5% CO_2 using a 24-well MEA system (Comfort; Alpha Med Scientific; recording electrode size 50 × 50 μm, recording electrode inter-electrode distance 150 μm, electrode impedance [f = 1 kHz] Typ. 10 kΩ) at a sampling rate of 20 kHz/channel. In the multiunit analysis, detected waveforms were first analyzed using the Presto and Mobius software (Alpha Med Scientific) and MATLAB. A spike was counted when the extracellular recorded signal exceeded a threshold of ±5.3 σ, where σ was the standard deviation of the baseline noise during quiescent periods.

2.4. Pharmacological tests

Organoids at 4 months of culture were placed in 24-well MEA plates. Spontaneous activities were measured after resting for 10 min in MEA. The organoids were collected immediately after the measurement completion. MEA recordings were obtained for 20 min after the application of a $GABA_A$-receptor antagonist—pentylenetetrazol (PTZ, 0.1, 0.3, 1, 3, 10 mM; P0046, Tokyo chemical Industry), glycine receptor antagonist—strychnine (3, 10, 30, 100 μM; S0632-5G, sigma), Na^+-channel blocker—phenytoin (3, 10, 30, 100, 300 μM; 166–12082, Wako), and AMPA-receptor antagonist—perampanel (0.03, 0.1, 0.3, 1, 3 μM; P285520, Toronto Research Chemicals).

2.5. Frequency analyses

Wavelet analysis was performed using a custom-written program in MATLAB (using function cwt in the package "Wavelet Toolbox"). Briefly, the raw data, $f(t)$, was transformed as follows:

$$W(b,a) = \frac{1}{\sqrt{a}} \int_{-\infty}^{\infty} f(t) G\left(\frac{t-b}{a}\right) dt$$

where a and b denoted the scaling factor (1/Hz) and the center location (ms) of the mother wavelet function, respectively. 1/a varied from 0.1 to 250 Hz. $G(x)$ is the complex Morlet function:

$$G(x) = \frac{1}{\sqrt{\pi F_B}} \exp\left(-\frac{x^2}{F_B}\right) \exp(2i\pi F_C x)$$

where $F_B = 5$ was the frequency bandwidth or wavenumber and $F_C = 1$ was the center frequency.

The wavelet power spectrum, W(b, a) was also specified. The amplitude of this transform was obtained from its absolute value and was color-coded. A scalogram is drawn with the Y axis representing the frequency band as 181 pixels and the X axis representing time. One pixel on the X axis is 50 μs.

$$WT_A = \frac{WT_S}{N_X \times N_Y(f)}$$

WT_A: Wavelet transform coefficient per pixel in each frequency band.

WT_S: Summation of wavelet transform coefficient in each frequency band.

N_X: Number of pixels on X axis.

$N_Y(f)$: Number of pixels on the Y axis, f is the frequency band.

The voltage peak value of the oscillation was detected from the raw waveform, but those with a peak value of ≤20 μV were excluded from the analysis. In addition, we calculated the frequency power at the

±250 ms of peak time and created the scalogram of average in an oscillation for 80 s.

3. Results

3.1. Structure of cerebral organoids derived from human iPSCs

To investigate organoids functionally, we were measured spontaneous activities and pharmacological response using the MEA system (Fig. 1A–a). We made cerebral organoids derived from human iPSCs and investigated neuronal differentiation characteristics using immunocytochemistry (Fig. 1A and b). Sliced samples were dyed using Hoechst 33,258 as a cell nuclear marker, PAX6 as an unspecialized cells marker, β-tubulin III as a neuronal marker, and ctip2 as a cortical marker. Immunocytochemistry showed that β-tubulin III and ctip2 were expressed in organoids. These results suggested that the produced organoids contain the basic components in a developing human cerebral cortex *in vitro* model, indicating that human cerebral organoids have a functional structure.

3.2. Frequency analysis of electrical activities in cerebral organoids after convulsant administration

Spontaneous activities were measured in cerebral organoids on a 24-

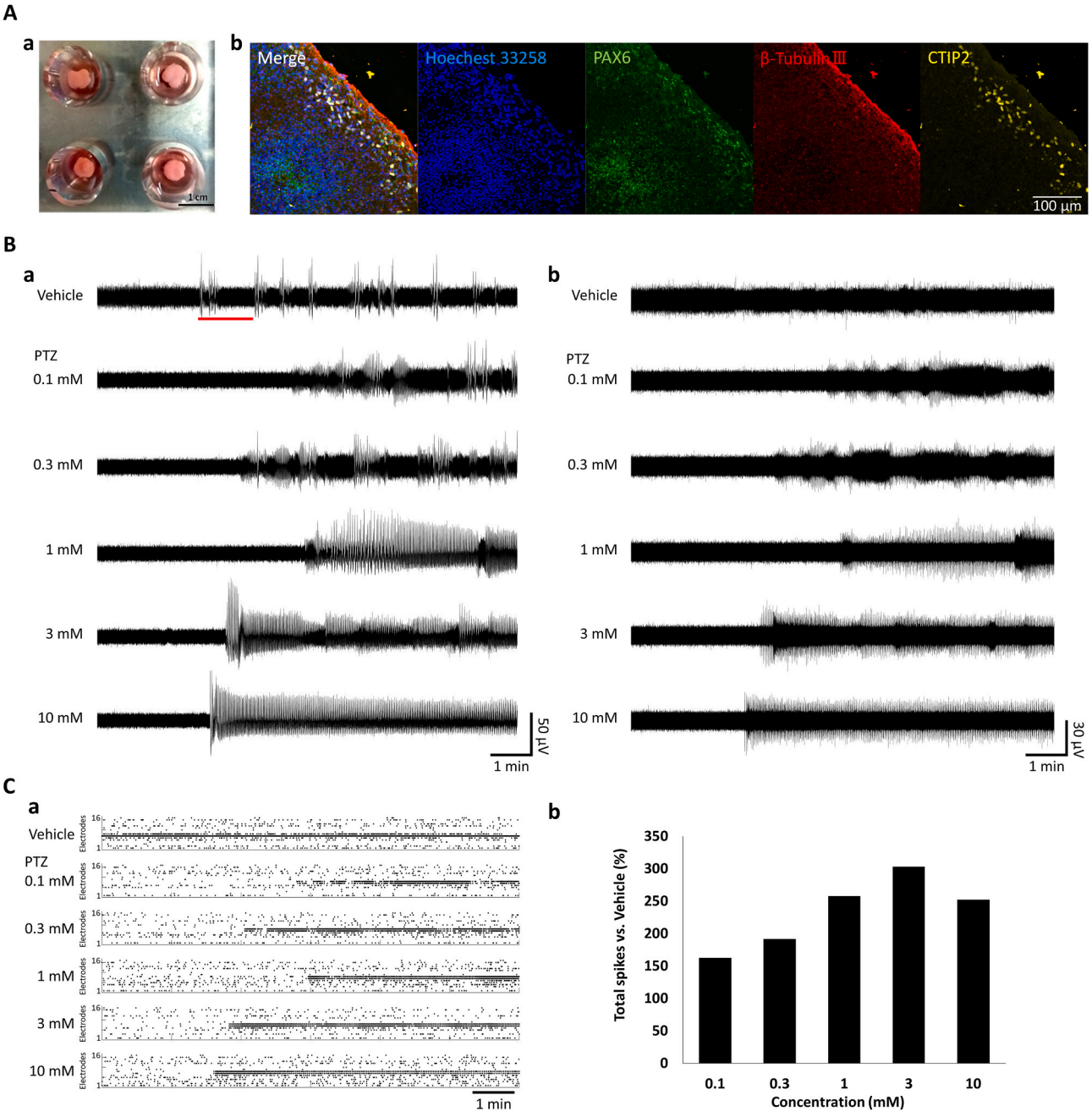

Fig. 1. Microelectrode array (MEA) recording to pentylenetetrazol (PTZ) administration in 4-month cerebral organoids.
(A) a: Brain organoid on MEA. b: Characterization of brain organoids by immunocytochemistry. Hoechst 33, 258 (blue), aired box protein 6 (PAX6, green), β-Tubulin III (red), CTIP2 (yellow). (B) Spontaneous activities after 10 min in PTZ administration. a: Spontaneous activities raw waveforms. b: Waveforms with components below 100 Hz removed in a high-pass filter. (C) Changes in multiunit activities after PTZ administration. a: Raster plots in all 16 electrodes. b: Change in the total number of spikes versus vehicle. . (For interpretation of the references to color in this figure legend, the reader is referred to the Web version of this article.)

well MEA chip. In addition, we used PTZ typical convulsant to obtain drug response. Fig. 1B (a) shows spontaneous activities raw waveform after 10 min of PTZ administration and Fig. 1B (b) shows that the raw waveform in Fig. 1B (a) is cut on components below 100 Hz using a high-pass filter. The spontaneous activities are observed in vehicle administration (Fig. 1 B-a). The frequency of electrical activities and amplitude were increased in a concentration-dependent manner after PTZ administration in the raw waveform and frequency components (Fig. 1B–a). The sustained response was observed immediately over 4 min after the first single oscillation in 1, 3, and 10 mM PTZ administration (Fig. 1B–a, b). These sudden and sustained firings are activities not found in the cultured neuronal network.

Fig. 1C (a) of the histogram shows the raster plot of spontaneous firing at 16 electrodes per 1 s after PTZ administration. Fig. 1C (b) shows the rate of change in the number of spikes for 10 min after normalization in the vehicle using a multiunit analysis. The total spike rate normalized by vehicle concentration increased to 162.7% at 0.1 mM, 191.9% at 0.3 μM, 258% at 1 μM, 303.2% at 3 μM, and 252.2% at 10 μM. The multiunit analysis showed a concentration-dependent increase in the number of firings, but it was not sufficiently extracted from the change in waveforms. Therefore, we investigated the characteristics of frequency components below 500 kHz (Fig. 2).

Fig. 2A shows raw waveforms and wavelet analysis between 0.3 and 9 Hz for 5 min before and after PTZ administration. As shown in the scalograms presented in Fig. 2A (a), oscillations were discrete in vehicles at 0.1 and 0.3 mM. In 0.1 and 0.3 mM PTZ, oscillations fluctuating from 1 to 3 Hz were observed at intervals of 30–40 s. Over a PTZ concentration of 1 mM, oscillations changed more persistently and periodically (Fig. 2 A-a). In addition, the first oscillation in 3 mM and 10 mM PTZ showed strong frequency components. Fig. 2A and b indicates the frequency power histograms of the red line part in Fig. 2A (a). In the total value of oscillation frequency, peak power at peak frequency were 1661.49 at 1.41 Hz (vehicle), 1430.84 at 1.41 Hz (0.1 mM), 1542.90 at 1.41 Hz (0.3 mM), 5474.25 at 1.26 Hz (1 mM), 3089.08 at 1.12 Hz (3 mM), and 5735.20 at 0.89 Hz (10 mM). The frequency power showed a marked increase from 1 mM. These results also show sustained and periodical activities, depending on the concentration of PTZ.

To investigate the characteristic of one oscillation, we detected oscillation from raw waveform (red dot in Fig. 2 B-a) and investigated the average of frequency power at 4–500 Hz in one oscillation at each concentration (Fig. 2 B-b). The power of frequency at 4–10 Hz increased in PTZ administration. The power of oscillation also increased (60–460 Hz) in a concentration-dependent manner (Fig. 2 B-b). In particular, the 100–300 Hz band was enhanced at 3 and 10 mM. Furthermore, the duration of the increased power of frequency was approximately 250 ms at 3 and 10 mM (Fig. 2 B-b). In summary, the strength of 4–10 Hz and 60–460 Hz was increased in one oscillation. Thus, the frequency components are contained the information of responses to PTZ and detailed information can be obtained by analyzing each oscillation.

Next, we investigated whether cerebral organoids respond to drugs having other mechanisms of action. Fig. 3 shows the raw waveform and wavelet analysis of electrical activities after 5 min after strychnine administration. The number of oscillations was 4 for the vehicle, 2 at 0.3 μM, 6 at 1 μM, 3 at 3 μM, 22 at 10 μM, and 8 at 30 μM. At 10 μM, the number of oscillations was clearly increased and sustained oscillations were observed. The wavelet analysis showed that the frequency band of 4–10 Hz increased in strychnine administration and that of 4–500 Hz also increased in 10 μM. Strychnine is a glycine and acetylcholine receptor antagonist. Thus, glycine receptor may express and function in organoids.

The results showed a concentration-dependent seizure-like waveform with sustained neural activities of GABA-A receptor antagonist upon PTZ administration. Furthermore, the information was listed on low frequencies with both PTZ and strychnine.

3.3. Responses to AEDs in cerebral organoids

We measured electrical activities in responses to perampanel and phenytoin administrations in 4-month cerebral organoids to investigate their response to anticonvulsants. In the raw waveform for 10 min after perampanel administration, the oscillation frequency decreased in a concentration-dependent manner and disappeared at 1 and 3 μM (Fig. 4A–a). Fig. 4B and C shows representative raster plots and the total number of spikes after AED administration for 10 min. In the case of the perampanel administration, the total number of spikes normalized by the vehicle decreased in a concentration-dependent manner to 64.0%, 29.4%, 10.4%, 6.54%, and 5.64% at 0.03, 0.1, 0.3, 1, and 3 μM, respectively (Fig. 4B–a and C-a). In the case of phenytoin administration, the number of spikes did not decrease till the concentration of 30 μM but a group of synchronized bursts occurred from 10 μM (Fig. 4A–b and B-b). Total spikes were decreased to 47.3% at 100 μM and 2.12% at 300 μM (Fig. 4C–b). Fig. 4D shows a characteristic raw oscillation waveform of the red line in Fig. 4A and the results of wavelet analysis. Recurring activities were observed after a single oscillation between both organoid samples (Fig. 4D). Frequency components near 10–30 Hz were raised after the oscillation, which indicated that there are recurring activities. The power of recurring activities decreased in a concentration-dependent manner in the case of perampanel and phenytoin administrations. Furthermore, the oscillation width decreased in a concentration-dependent manner in phenytoin. In summary, recurring activity was observed in the case of both drugs in vehicle administration and it was listed in the wavelet waveform. Moreover, we observed reduced power in the case of one oscillation in both drugs. In the case of perampanel, the oscillations were only reduced. However, in the case of phenytoin, the oscillation frequency increased. Therefore, the phenomenon of decreased recurring activity after oscillation was potentially similar but their appearance varied between perampanel and phenytoin.

4. Discussion

We demonstrated the recording of electrical activities in human iPSC-derived cerebral organoids using MEA and detected the electrical activity characteristics of organoids in frequency components. A measuring device is also important for acquiring frequency components. The frequency components could be analyzed because an MEA system with low impedance electrodes was used.

We observed a concentration-dependent seizure-like waveform with sustained neural activities in the case of PTZ and strychnine administration (Figs. 1B, 2 and 3). Moreover, there was a concentration-dependent increase in the multiunit activity (Fig. 1C–b). In EEG of rats, the multiunit activity is increased in the oral administration of PTZ [25]. Therefore, these results suggested that the electrical activities from organoids are similar to those in mammals. After PTZ administration, sudden and sustained firings were observed in this organoid study. In the case of cultured human iPSC-derived neurons, network bursts were observed before drug administration and the frequency of network bursts was reported to increase with PTZ administration [26]. Therefore, the sudden and sustained firings observed in the organoids are considered to be the characteristic phenomena not found in cultured neuronal networks.

The peak power calculated from these total values of oscillation frequency was also increased upon 1, 3, and 10 mM PTZ administrations. The intensity of the band below 10 Hz showed a concentration-dependent increase. The intensity of the 60–460 Hz band was increased and widespread in the cases of 1, 3, and 10 mM PTZ administrations (Fig. 2B). In particular, the 100–300 Hz band was enhanced at 3 and 10 mM (Fig. 2B–b). Analysis of frequency components of cerebral organoids below 500 Hz is considered an effective method for predicting the seizure liability of drugs.

In the EEGs of epilepsy patients, 80–500 Hz is used as a marker for

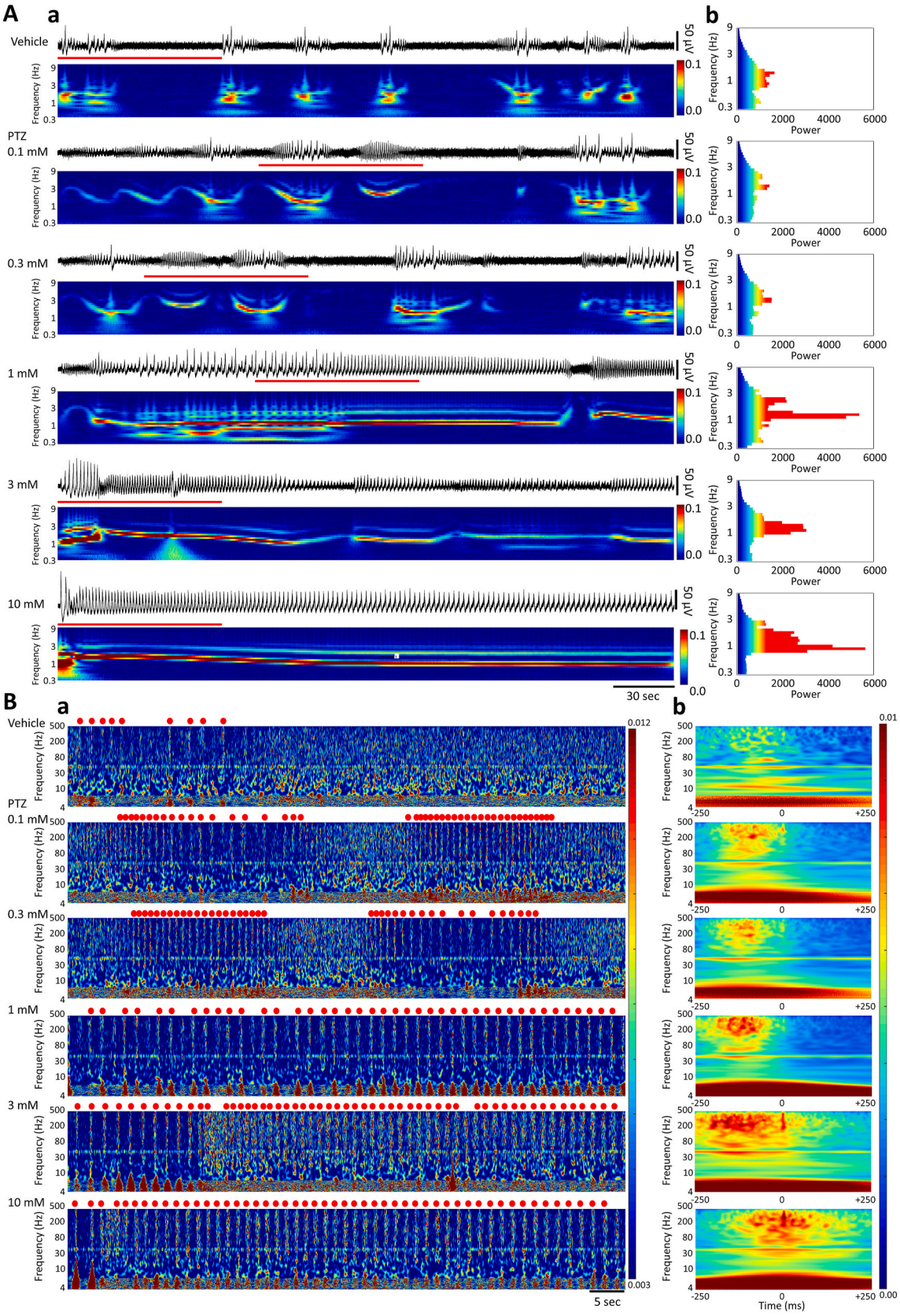

Fig. 2. Frequency analysis below 500 Hz in PTZ administration.
(A) a: Raw waveforms for 5 min and the scalogram of 0.3–9 Hz. Enlarged view of red line part in Fig. 1B a. b: The histogram of frequency power in 0.3–9 Hz. (B) a: Scalogram of 4–500 Hz for 80 s in the red line part of A-a. Red dots indicate detected synchronized activities. b: Average value of frequency power in detected synchronized activities. The scalogram with peak detection time ±250 ms. Vehicle (n = 9), 0.1 mM (n = 44), 0.3 mM (n = 39), 1 mM (n = 41), 3 mM (n = 55), 10 mM (n = 51). . (For interpretation of the references to color in this figure legend, the reader is referred to the Web version of this article.)

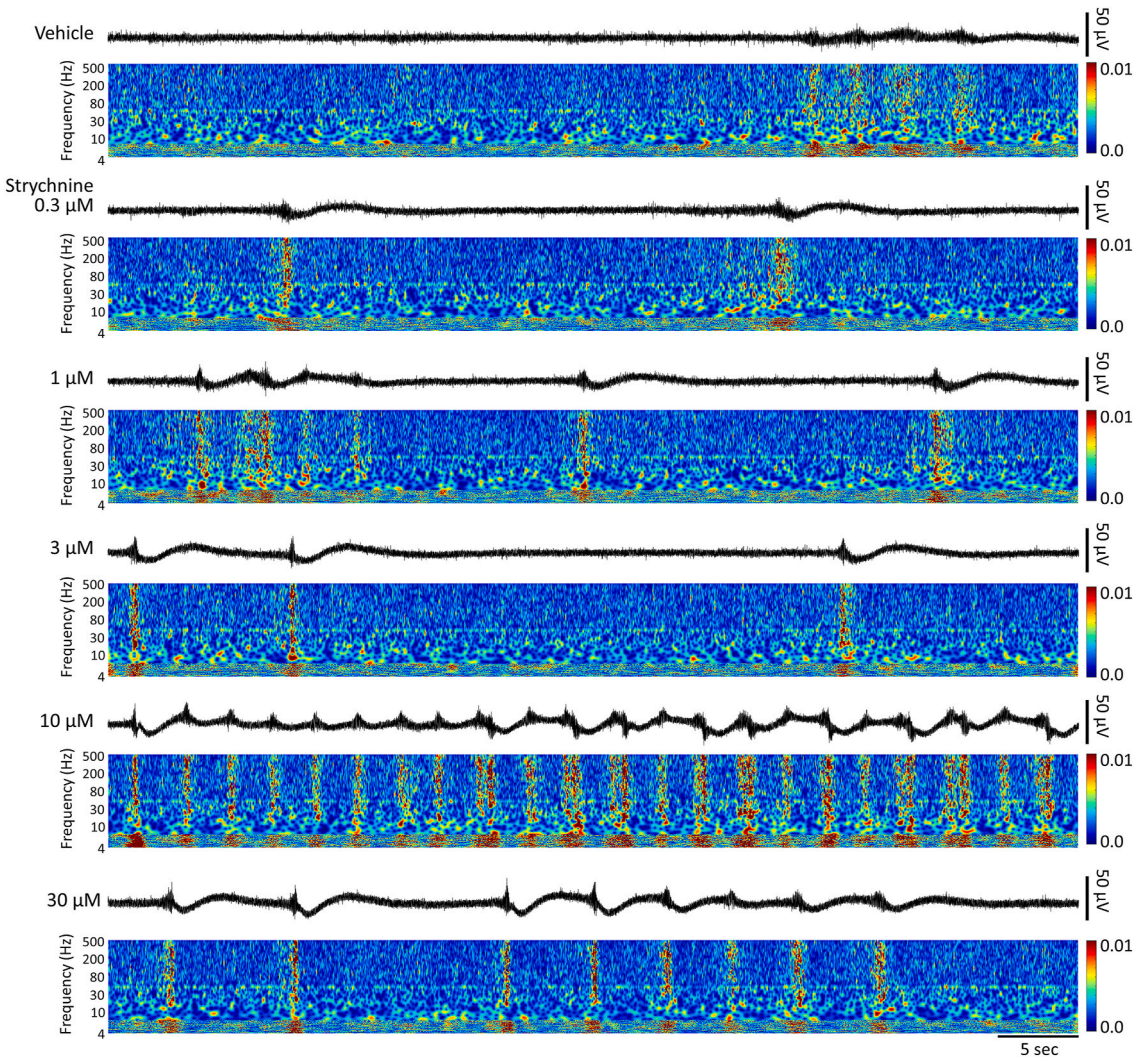

Fig. 3. Responses to strychnine in 4-month cerebral organoids.
Raw waveform and scalogram of electrical activities in strychnine administration. A wavelet analysis was computed of the characteristic raw waveform (4–500 Hz) for 60 s in strychnine administration.

seizures [27]. Characteristic waveforms are observed in the frequency band of 100–300 Hz [28]. Below 100 Hz, the β and γ waves are enhanced in the EEGs of patients with epilepsy [29]. Childhood epilepsy has been reported to involve increased activity in the 3 Hz band [30]. In *in vivo* PTZ administration experiments using animal models, changes were reported in the 11 Hz band in dogs [31], 6 Hz band in rats and mice [31], and all bands below 50 Hz in cynomolgus monkeys [32]. In this study, we examined the possibility of evaluating the seizure liability of drugs using organoids, prepared organoids from healthy donor-derived iPSCs, and then detected the responses of the organoids to convulsants. As a result, the comparison of these findings with the *in vivo* EEG data of diseased patients is difficult. As the frequency characteristics observed in the EEGs of epilepsy patients vary depending on the disease type, future studies should examine whether disease-specific frequency characteristics can be detected using diseased brain organoids developed from patient-derived iPSCs. When seizure-like activities are observed in cerebral organoids prepared from diseased iPSCs, frequency analysis below 500 Hz, as shown in this study, is considered effective.

Perampanel is an AED mainly affecting the AMPA glutamate receptor. We observed synchronized bursts and the concentration-dependent decrease in the number of firings upon perampanel administration (Fig. 4A–a, 4C-a). In rats, we demonstrated that pilocarpine-induced epilepsy-like EEGs were suppressed by perampanel administration [33]. Moreover, phenytoin, an old-generation Na^+-channel blocker, remarkably decreased the number of firings in 100–300 μM (Fig. 4A and b). In rats transplanted with epidural electrodes, the induced epilepsy-like EEG following the intracortical administration of FeCL3 was suppressed upon phenytoin administration [34]. Moreover, epilepsy-like EEG is suppressed in humans by the oral administration of phenytoin [35]. Interestingly, we observed the occurrence of bursts-like seizures in the data related to phenytoin. Phenytoin displays reported side effects [36]. Therefore, the elevated bursts detected with organoids might reflect the side effects of phenytoin. The wavelet analysis showed a concentration-dependent decrease in the recurring activity upon perampanel and phenytoin administration (Fig. 4D–a,b). The synaptic transmission of the network might have been inhibited, and a recursive decrease in frequency power was observed. According to the results of this study, changes to AEDs can be evaluated using brain organoids, including organoids prepared from healthy donor-derived iPSCs. However, when evaluating AEDs, it would be ideal to test AEDs using organoids that show seizure-like activity. A future task will be to produce organoids that show seizure-like activity from iPSCs derived from patients.

These results indicated that we detected the change in electrical activities by convulsants and AEDs administration focusing on the frequency components below 500 Hz. However, the production of highly

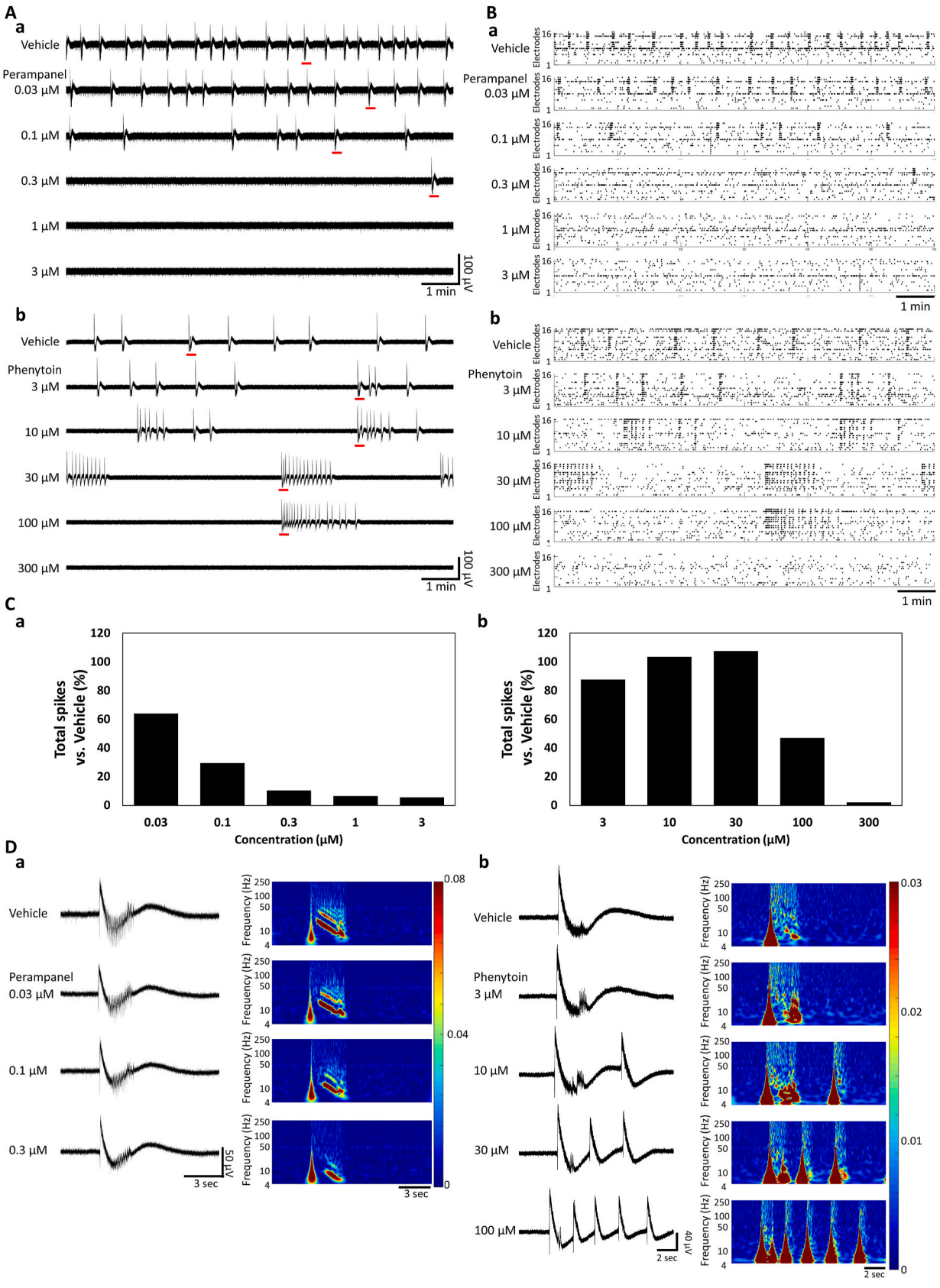

Fig. 4. Responses to antiepileptic drugs (AEDs) in 4-month cerebral organoids.
(A) Raw waveforms of spontaneous activities for 10 min in AEDs administration. (a) Perampanel. (b) Phenytoin. (B) Representative raster plots at all 16 electrodes for 10 min. (a) Perampanel. (b) Phenytoin. (C) Changes in multiunit activities. (a) Perampanel. (b) Phenytoin. (D) Frequency analysis in on oscillation in the red line part of A-a and b. The characteristic typical raw waveforms (left) and 4–250 Hz scalograms (Right) after AEDs administration for 15 s. (a) Perampanel. (b) Phenytoin. .
(For interpretation of the references to color in this figure legend, the reader is referred to the Web version of this article.)

reproducible cerebral organoids remains a challenge. The seizure-like response of organoids is not observed every time in PTZ administration (Fig. 1B). The stability of the firing pattern is considered to depend on the state of the produced organoids. Therefore, to build a stable evaluation system in the future, we need to clarify the relation between the state of produced organoids and electrical activity. Furthermore, in this study, the waveform could be observed byjust placing the organoid on the MEA chip without a weight. The obtained data represent signals from the surface of the organoid. To analyze the function of organoids in more detail using this system, we need to measure the electrical activity inside the organoid. Therefore, our next challenges would be to create organoid sections and measure electrical activities with their use.

In this study, analysis of the electrical activity of cerebral organoids revealed that frequency analysis below 500 Hz is effective. Our findings suggest that the analysis of frequency components of organoids is effective in the assessment of the seizure liability of drugs and effects of AEDs as well as for performing IVIVE. Frequency component analysis in MEA is expected to become an important analysis method for studying brain organoids in the future and can support scientific research on the function of the organoid itself, development of the human brain, and treatment of various diseases.

Declaration of competing interest

All authors have no conflicts of interest to declare.

Acknowledgments

This study was supported by JSPS KAKENHI Grant Numbers 20H04507, 20J23851 and the science research promotion fund.

References

[1] M.A. Lancaster, J.A. Knoblich, Organogenesis in a dish: modeling development and disease using organoid technologies, Science (New York, N.Y.) 345 (2014), 1247125.
[2] D. Dutta, I. Heo, H. Clevers, Disease modeling in stem cell-derived 3D organoid systems, Trends Mol. Med. 23 (2017) 393–410.
[3] S. Ramani, S.E. Crawford, S.E. Blutt, M.K. Estes, Human organoid cultures: transformative new tools for human virus studies, Current opinion in virology 29 (2018) 79–86.
[4] B.R. Dye, D.R. Hill, M.A. Ferguson, Y.H. Tsai, M.S. Nagy, R. Dyal, J.M. Wells, C. N. Mayhew, R. Nattiv, O.D. Klein, E.S. White, G.H. Deutsch, J.R. Spence, In vitro generation of human pluripotent stem cell derived lung organoids, eLife (2015) 4.
[5] I. Kelava, M.A. Lancaster, Dishing out mini-brains: current progress and future prospects in brain organoid research, Dev. Biol. 420 (2016) 199–209.
[6] H. Sakaguchi, T. Kadoshima, M. Soen, N. Narii, Y. Ishida, M. Ohgushi, J. Takahashi, M. Eiraku, Y. Sasai, Generation of functional hippocampal neurons from self-organizing human embryonic stem cell-derived dorsomedial telencephalic tissue, Nat. Commun. 6 (2015) 8896.
[7] J. Jo, Y. Xiao, A.X. Sun, E. Cukuroglu, H.D. Tran, J. Göke, Z.Y. Tan, T.Y. Saw, C. P. Tan, H. Lokman, Y. Lee, D. Kim, H.S. Ko, S.O. Kim, J.H. Park, N.J. Cho, T. M. Hyde, J.E. Kleinman, J.H. Shin, D.R. Weinberger, E.K. Tan, H.S. Je, H.H. Ng, Midbrain-like organoids from human pluripotent stem cells contain functional dopaminergic and Neuromelanin-Producing neurons, Cell stem cell 19 (2016) 248–257.
[8] T. Wataya, S. Ando, K. Muguruma, H. Ikeda, K. Watanabe, M. Eiraku, M. Kawada, J. Takahashi, N. Hashimoto, Y. Sasai, Minimization of exogenous signals in ES cell culture induces rostral hypothalamic differentiation, Proc. Natl. Acad. Sci. U. S. A. 105 (2008) 11796–11801.
[9] K. Muguruma, A. Nishiyama, H. Kawakami, K. Hashimoto, Y. Sasai, Self-organization of polarized cerebellar tissue in 3D culture of human pluripotent stem cells, Cell Rep. 10 (2015) 537–550.
[10] H. Suga, T. Kadoshima, M. Minaguchi, M. Ohgushi, M. Soen, T. Nakano, N. Takata, T. Wataya, K. Muguruma, H. Miyoshi, S. Yonemura, Y. Oiso, Y. Sasai, Self-formation of functional adenohypophysis in three-dimensional culture, Nature 480 (2011) 57–62.
[11] K.L. Franson, D.P. Hay, V. Neppe, W.Y. Dahdal, W.U. Mirza, G.T. Grossberg, D. M. Chatel, P.A. Szwabo, S. Kotegal, Drug-induced seizures in the elderly. Causative agents and optimal management, Drugs Aging 7 (1995) 38–48.
[12] R. Roberts, S. Authier, R.D. Mellon, M. Morton, I. Suzuki, R.B. Tjalkens, J. P. Valentin, J.B. Pierson, Can We Panelize seizure? Toxicol. Sci. : an official journal of the Society of Toxicology 179 (2021) 3–13.
[13] R. Hanaya, K. Arita, The new antiepileptic drugs: Their Neuropharmacology and Clinical Indications, Neurol. Med.-Chir. 56 (2016) 205–220.
[14] A.I. Grainger, M.C. King, D.A. Nagel, H.R. Parri, M.D. Coleman, E.J. Hill, In vitro models for seizure-Liability Testing using induced pluripotent stem cells, Front. Neurosci. 12 (2018) 590.
[15] A. Odawara, N. Matsuda, Y. Ishibashi, R. Yokoi, I. Suzuki, Toxicological evaluation of convulsant and anticonvulsant drugs in human induced pluripotent stem cell-derived cortical neuronal networks using an MEA system, Sci. Rep. 8 (2018) 10416.
[16] T. Shirakawa, I. Suzuki, Approach to Neurotoxicity using human iPSC neurons: Consortium for safety assessment using human iPS cells, Curr. Pharmaceut. Biotechnol. 21 (2020) 780–786.
[17] G. Sun, F. Chiuppesi, X. Chen, C. Wang, E. Tian, J. Nguyen, M. Kha, D. Trinh, H. Zhang, M.C. Marchetto, H. Song, G.L. Ming, F.H. Gage, D.J. Diamond, F. Wussow, Y. Shi, Modeling human Cytomegalovirus-induced Microcephaly in human iPSC-derived brain organoids, cell reports, Medicine 1 (2020), 100002.
[18] A. Kathuria, K. Lopez-Lengowski, S.S. Jagtap, D. McPhie, R.H. Perlis, B.M. Cohen, R. Karmacharya, Transcriptomic landscape and functional characterization of induced pluripotent stem cell-derived cerebral organoids in schizophrenia, JAMA psychiatry 77 (2020) 745–754.
[19] H. Shin, S. Jeong, J.H. Lee, W. Sun, N. Choi, I.J. Cho, 3D high-density microelectrode array with optical stimulation and drug delivery for investigating neural circuit dynamics, Nat. Commun. 12 (2021) 492.
[20] H. Yao, W. Wu, I. Cerf, H.W. Zhao, J. Wang, P.D. Negraes, A.R. Muotri, G. G. Haddad, Methadone interrupts neural growth and function in human cortical organoids, Stem Cell Res. 49 (2020), 102065.
[21] S.R. Fair, D. Julian, A.M. Hartlaub, S.T. Pusuluri, G. Malik, T.L. Summerfied, G. Zhao, A.B. Hester, W.E.t. Ackerman, E.W. Hollingsworth, M. Ali, C.A. McElroy, I.A. Buhimschi, J. Imitola, N.L. Maitre, T.A. Bedrosian, M.E. Hester, Electrophysiological maturation of cerebral organoids Correlates with dynamic Morphological and Cellular development, Stem cell reports 15 (2020) 855–868.
[22] C.A. Trujillo, J.W. Adams, P.D. Negraes, C. Carromeu, L. Tejwani, A. Acab, B. Tsuda, C.A. Thomas, N. Sodhi, K.M. Fichter, S. Romero, F. Zanella, T. J. Sejnowski, H. Ulrich, A.R. Muotri, Pharmacological reversal of synaptic and network pathology in human MECP2-KO neurons and cortical organoids, EMBO Mol. Med. 13 (2021), e12523.
[23] D. Wang, Y. Shan, F. Bartolomei, P. Kahane, Y. An, M. Li, H. Zhang, X. Fan, S. Ou, Y. Yang, P. Wei, C. Lu, Y. Wang, J. Du, L. Ren, Y. Wang, G. Zhao, Electrophysiological properties and seizure networks in hypothalamic hamartoma, Annals of clinical and translational neurology 7 (2020) 653–666.
[24] E. Urrestarazu, J.D. Jirsch, P. LeVan, J. Hall, M. Avoli, F. Dubeau, J. Gotman, High-frequency intracerebral EEG activity (100-500 Hz) following interictal spikes, Epilepsia 47 (2006) 1465–1476.
[25] S.A. Lee, D.D. Spencer, S.S. Spencer, Intracranial EEG seizure-onset patterns in neocortical epilepsy, Epilepsia 41 (2000) 297–307.
[26] A. Odawara, H. Katoh, N. Matsuda, I. Suzuki, Physiological maturation and drug responses of human induced pluripotent stem cell-derived cortical neuronal networks in long-term culture, Sci. Rep. 6 (2016) 26181.
[27] M. Lévesque, A. Bortel, J. Gotman, M. Avoli, High-frequency (80-500 Hz) oscillations and epileptogenesis in temporal lobe epilepsy, Neurobiol. Dis. 42 (2011) 231–241.
[28] H. Khosravani, N. Mehrotra, M. Rigby, W.J. Hader, C.R. Pinnegar, N. Pillay, S. Wiebe, P. Federico, Spatial localization and time-dependant changes of electrographic high frequency oscillations in human temporal lobe epilepsy, Epilepsia 50 (2009) 605–616.
[29] M. Niknazar, S.R. Mousavi, B.V. Vahdat, M. Sayyah, A new framework based on recurrence quantification analysis for epileptic seizure detection, IEEE journal of biomedical and health informatics 17 (2013) 572–578.
[30] S.J. Smith, EEG in the diagnosis, classification, and management of patients with epilepsy, J. Neurol. Neurosurg. Psychiatr. 76 (Suppl 2) (2005) ii2–7.
[31] S. Authier, J. Arezzo, M. Pouliot, M.V. Accardi, E. Boulay, E. Troncy, M. Dubuc Mageau, W. Tan, A. Sanfacon, S. Mignault Goulet, D. Paquette, EEG: characteristics of drug-induced seizures in rats, dogs and non-human primates, J. Pharmacol. Toxicol. Methods 97 (2019) 52–58.
[32] C.S. Metcalf, P.J. West, K.E. Thomson, S.F. Edwards, M.D. Smith, H.S. White, K. S. Wilcox, Development and pharmacologic characterization of the rat 6 Hz model of partial seizures, Epilepsia 58 (2017) 1073–1084.
[33] H. Mohammad, S. Sekar, Z. Wei, F. Moien-Afshari, C. Taghibiglou, Perampanel but not Amantadine Prevents behavioral Alterations and epileptogenesis in pilocarpine rat model of status Epilepticus, Mol. Neurobiol. 56 (2019) 2508–2523.
[34] A.K. Srivastava, S.K. Gupta, S. Jain, Y.K. Gupta, Effect of melatonin and phenytoin on an intracortical ferric chloride model of posttraumatic seizures in rats, Methods Find Exp. Clin. Pharmacol. 24 (2002) 145–149.
[35] M. Fink, P. Irwin, W. Sannita, Y. Papakostas, M.A. Green, Phenytoin: EEG effects and plasma levels in volunteers, Ther. Drug Monit. 1 (1979) 93–103.
[36] T. Antoniou, T. Gomes, M.M. Mamdani, D.N. Juurlink, Trimethoprim/sulfamethoxazole-induced phenytoin toxicity in the elderly: a population-based study, Br. J. Clin. Pharmacol. 71 (2011) 544–549.